FERMI NATIONAL
ACCELERATOR LABORATORY

TECHNICAL DIVISION
SRF DEPARTMENT

FINAL REPORT

Design of the insertion tooling for the SSR1 cryomodule

Author:
Cecilia Moreschini

Primary Supervisor:
Vincent Roger
Alternate Supervisor:
Donato Passarelli

Summer Internship 2018

Abstract

Proton Improvement Plan-II (PIP-II) is Fermilab's plan for providing powerful, high-intensity proton beams to the laboratory's experiments. The increased beam power will position Fermilab as the leading laboratory in the world for accelerator-based neutrino experiments. The heart of PIP-II is a 800-MeV superconducting linear accelerator which consists of five different SRF cavity types: half wave resonator (HWR), 325 MHz single spoke resonators (SSR1, SSR2), 650 MHz multicell cavities (LB650, HB650).
In this report is described the design and development of part of the insertion tooling for the assembly of the SSR1 cryomodule.

Contents

1 Introduction

1.1 Description of the SSR1 cryomodule

The cavity string assembly of the SSR1 cryomodule is made up of eight single spoke resonators type 1 and four superconducting solenoids in sequence C-S-CC-S-CC-S-CC-S-C.
All the cavities and magnets are mounted to the support posts using adjustable positioning mechanism. The support posts are fixed to a full-length (about 5 m) aluminum strongback located between the vacuum vessel and thermal shield. The design of the thermal shield and support posts is such that the strongback remains at room temperature while the active components are at 2 K. This solution preserves the precise alignment of the cavities and solenoids performed prior to the insertion of the coldmass unit into the vacuum vessel for the final assembly.
In Fig. 1 are shown some of the main parts of the SSR1 cryomodule.

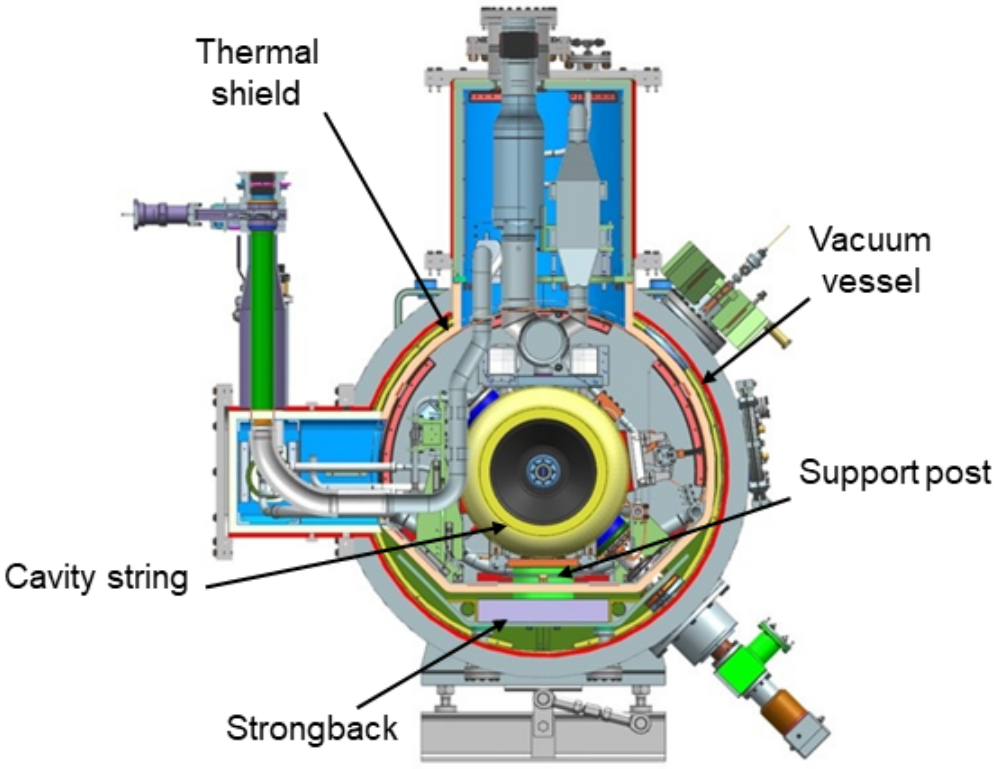

Figure 1: Cross-section of the SSR1 cryomodule

1.2 Assembly Process

The first SSR1 cryomodule for PIP-II will be assembled in the Fermilab Lab 2 facility starting from the cavity string assembly in a class 10 (ISO 4) cleanroom to the final cryomodule assembly. The assembly procedure is divided into many phases, the main ones are shown in Fig. 2.
The insertion tooling which has been developed concerns the insertion of the coldmass assembly into the vacuum vessel (Fig. 2g).

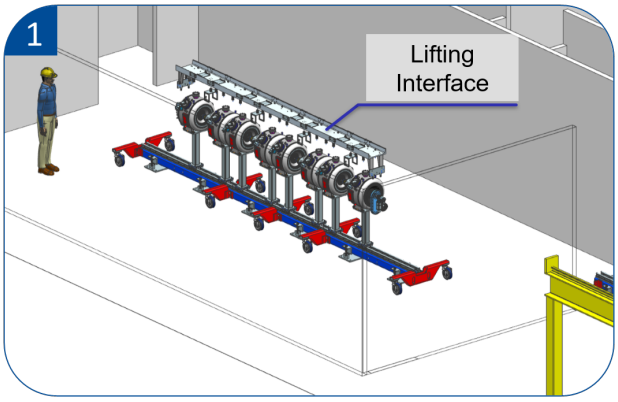

(a) Installation of the cavity string lifting interface

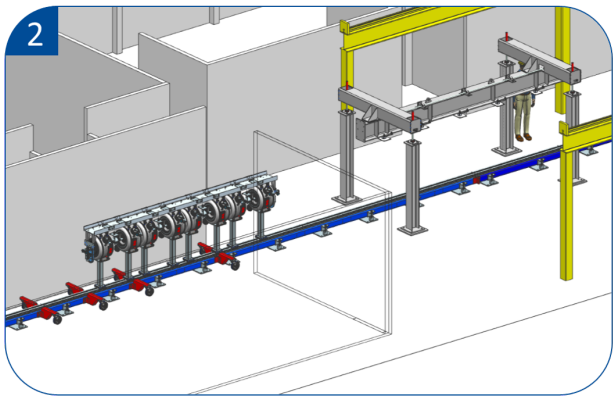

(b) Transportation of the cavity string to the assembling area

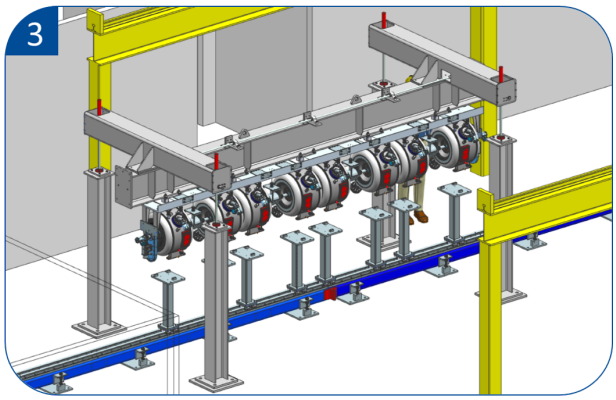

(c) Cavity string lifting from the cavity string support posts

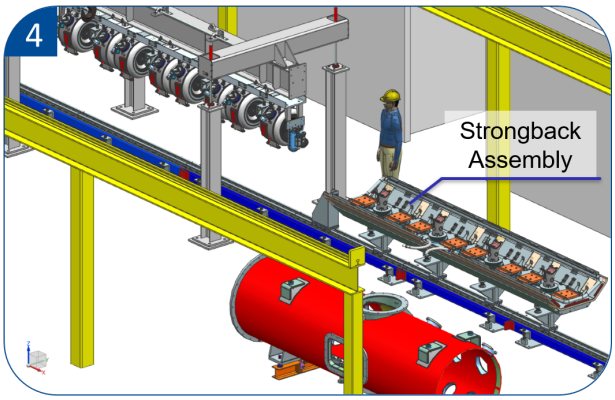

(d) Strongback assembling onto the coldmass support posts

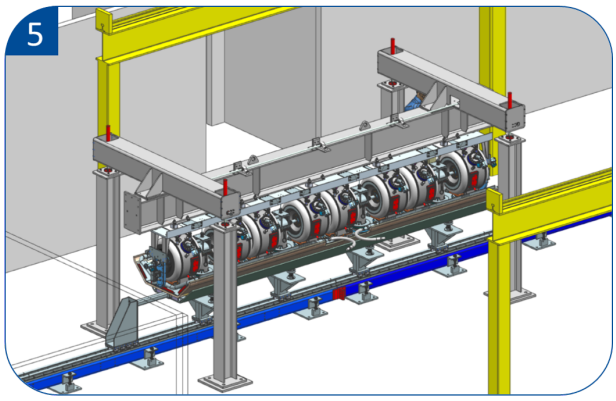

(e) Installation of the cavity string onto the strongback assembly

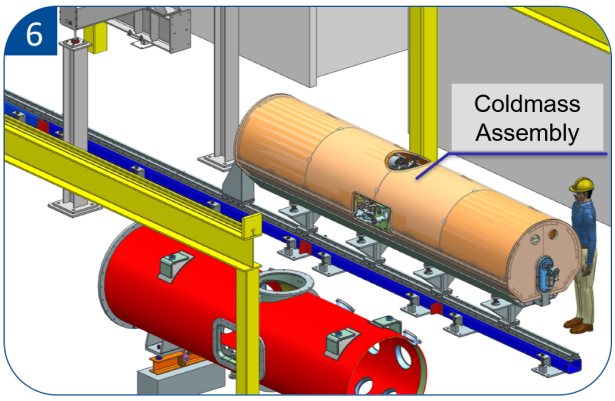

(f) Completion of the coldmass assembly

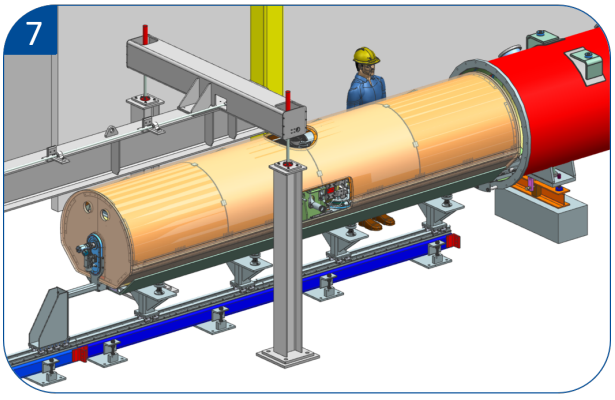

(g) Insertion of the coldmass assembly into the vacuum vessel

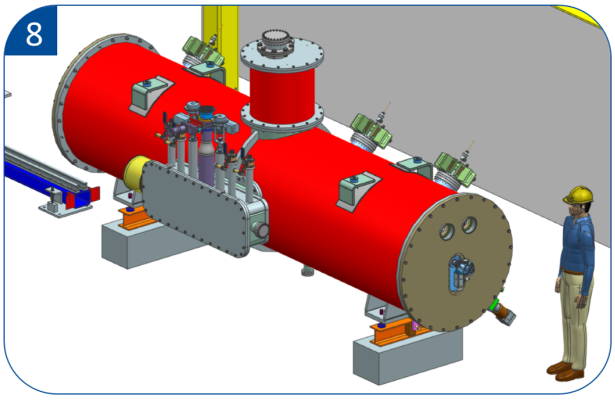

(h) Completion of the cryomodule assembly

Figure 2: Main phases of the SSR1 cryomodule assembling procedure

2 Previous studies of the insertion tooling

During the last years, many studies have been done in order to allow the insertion of the coldmass into the vacuum vessel. A conveyor roller has been designed and verified performing several simulations. This system is made up of several rollers with a suitable housing. The conveyor roller shown in Fig. 3 is installed inside the vacuum vessel prior the insertion. Then, the coldmass is inserted above its nominal position. A hydraulic lifting system has been integrated into the insertion tooling to move down the coldmass on the vacuum vessel supports and finally to pull out the tooling from the vacuum vessel. This last step is the critical one: the small clearance (2-3 mm) between the roller system and the strongback cannot guarantee a safely removal of the conveyor and cannot prevent difficulties in the extraction.

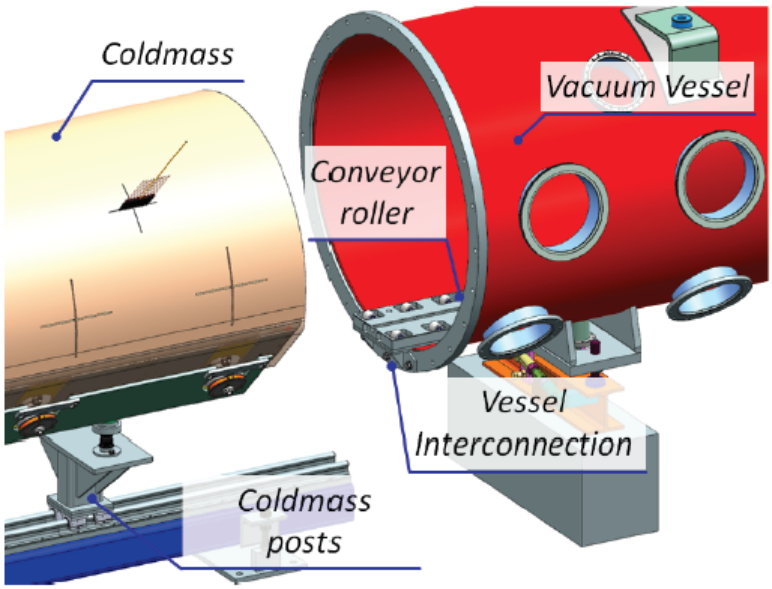

Figure 3: Insertion tooling of the coldmass into the vacuum vessel

In order to avoid the problems described above, a different strategy has been conceived (Fig. 4). The aim of this solution is to make the insertion as simpler as possible using just few tools: one hook bracket to be connected to an adjustable support with mechanical actuator and a back bracket with a wheel that will allow the relative motion between the strongback and the vacuum vessel.
At the beginning of the process the strongback is held up by eight supports (Fig. 4a). Then the coldmass assembly is inserted thanks to a rail system and the supports are removed, one by one (Fig. 4b). At the end of the procedure the strongback is supported just by the ends, thanks to the two brackets connected to adjustable supports (Fig. 4c). Once the insertion is completed the adjustable supports are lowered down and the strongback sits on the eight supports of the vessel (Fig. 4d).

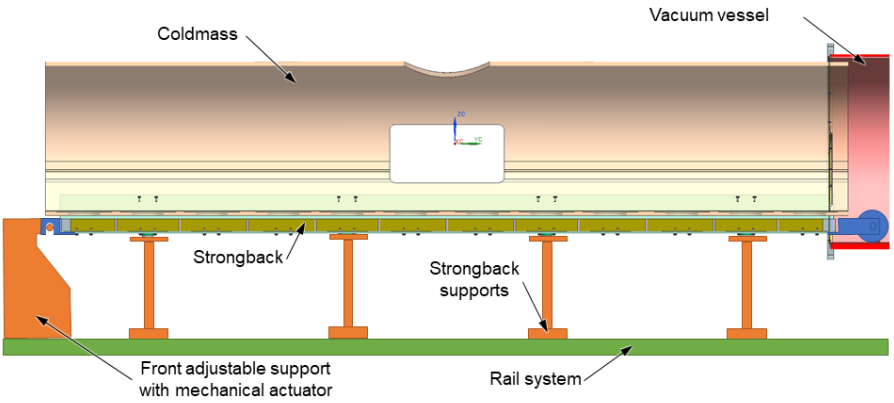

(a) The coldmass assembly is held up by eight supports

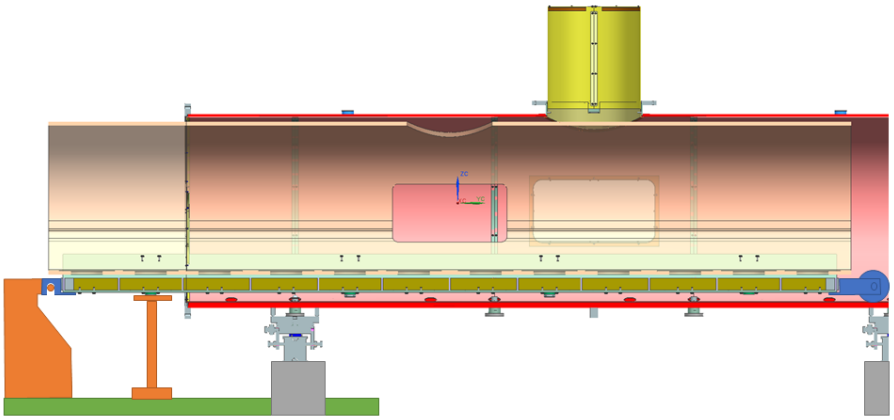

(b) The vacuum vessel is slided thanks to a rail system

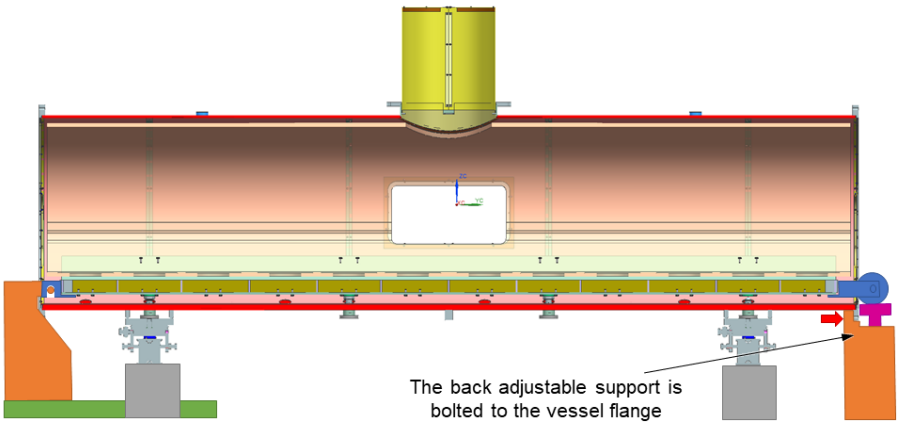

(c) End of the insertion: the coldmass assembly is supported just by the ends

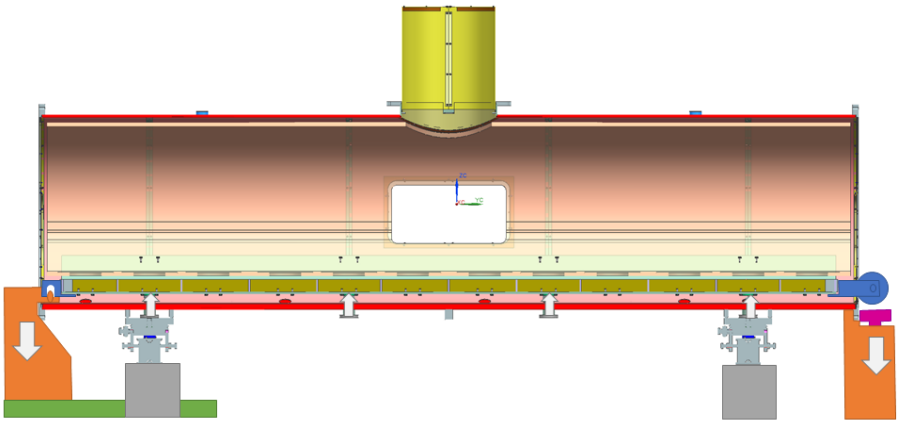

(d) The adjustable supports are lowered down and the coldmass assembly sits on the eight supports of the vessel

Figure 4: Coldmass installation fixture

3 Validation of the coldmass installation fixture

Just before lowering down the adjustable supports the strongback is supported only by the ends: this is the configuration in which the maximum deflection is expected.
Finite Elements Analyses using ANSYS® Workbench have been performed in order to estimate the vertical deflection. The coldmass weight (28.8 kN) and the gravity are applied as vertical loads. Just half of the structure is simulated because of the symmetry of the model. A symmetrical boundary condition is applied to the middle section of the strongback (plane x-y in Fig. 6) while there are no constraints in the axial z direction.
The maximum deflection shown by the first analysis is about 12 mm. This deflection is such that it could provoke misalignments of the cavities after the insertion. In order to reduce that value, changes to the strongback geometry have been suggested. It is worth to notice that the strongback is already in Fermilab Lab 2 facility: the strongback shape cannot be overturned and it is better to machine the strongback as little as possible. Therefore, the best solution to stiffen the structure is to weld aluminum parts, trying to increase its second moment of inertia.
A first calculation has been performed by stiffening the strongback using L brackets and plates (Fig. 5). The welded surfaces are modelled as bonded contacts. In that way the deflection goes down to 7 mm as shown in Fig. 6a.
In order to further decrease the deflection, new modifications have been suggested on the upper surface of the strongback, welding aluminum parts and adding another row of steel ribs. Then, another simulation has been performed and the maximum deflection has been reduced to 4.3 mm (Fig. 6b). Even if the deflection is quite lower than initially, 4.3 mm could still be too much to prevent misalignments of the cavities.

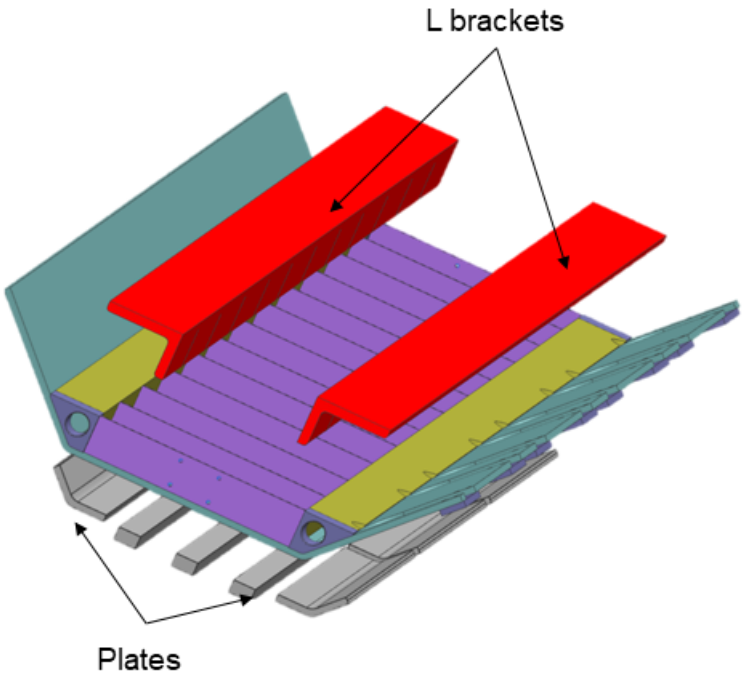

Figure 5: Exploded view of the first stiffened structure

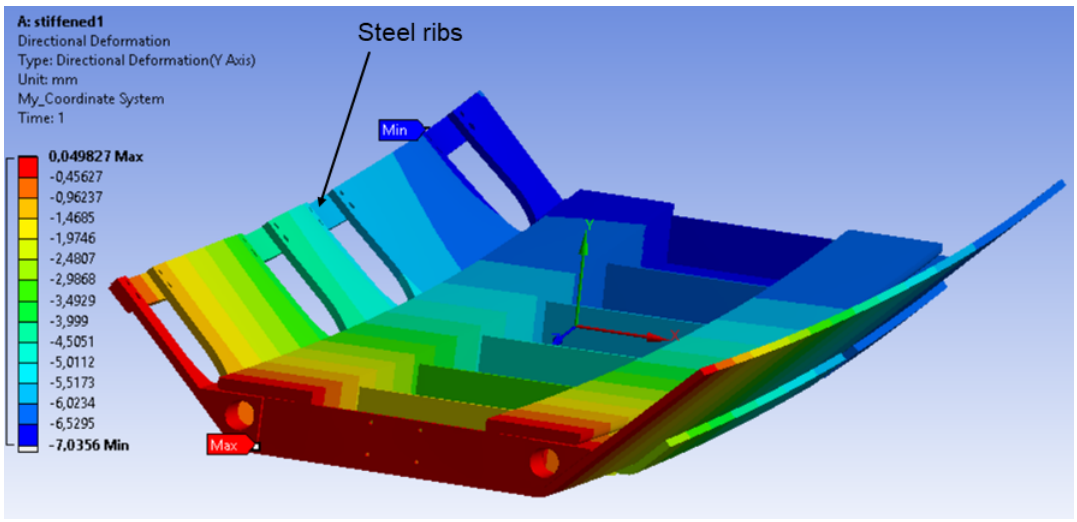

(a) Simulation of the first stiffened structure. Max. def. = 7 mm

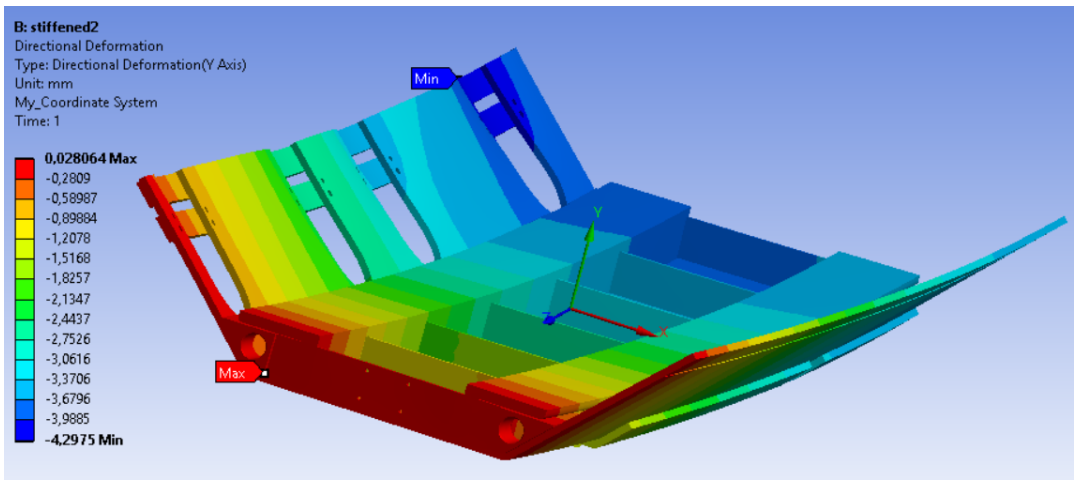

(b) Simulation of the final stiffened structure. Max. def. = 4.3 mm

Figure 6: FEM analysis of the stiffened strongback

4 New proposal of insertion tooling

The possibility to support the strongback just by the ends has been explored and the simulations performed have shown that the reliability is not guaranteed by this kind of insertion fixture. A different way to support and insert the strongback must be considered. Taking into account the problems related to the conveyor roller developed in last years, it has been decided to design a new roller system.

4.1 Main idea

The preliminary design of the new roller system (Fig. 7) consists of a standard rectangular steel tube connected to the lower surface of the strongback with screws. Stainless steel rollers are fixed to the tube in order to slide the whole system into the vacuum vessel under its nominal position. After the complete insertion, eight threaded supports are moved up until they are in contact with the strongback. Then the screws connecting the tube to the strongback are unfastened, the strongback is set to its nominal position using the threaded supports and the roller system can be removed. The steps of the insertion process are described in more detail in Section 5.

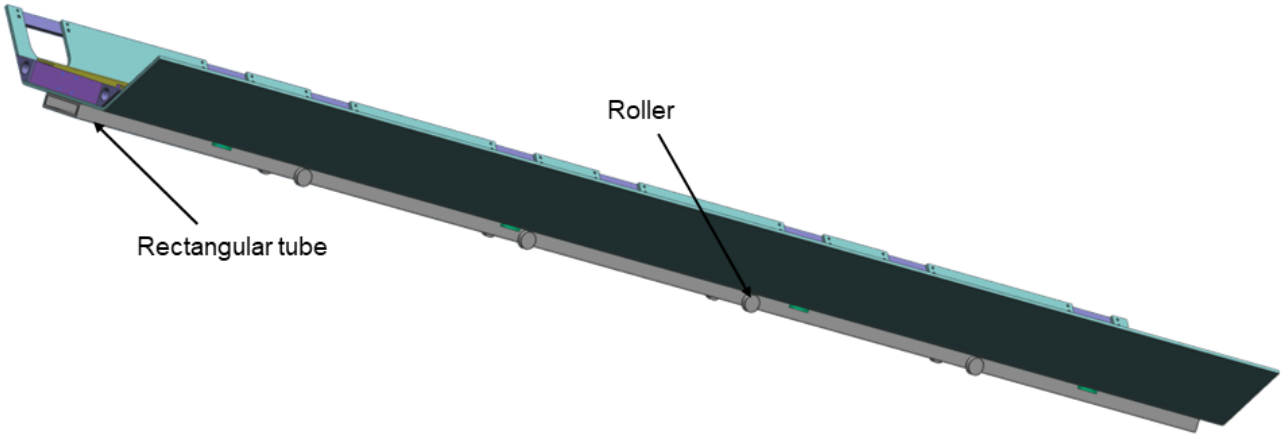

Figure 7: Preliminary design of the roller system connected to the strongback

4.2 First step of the lifting procedure

Before proceeding to develop the design of the roller system, it has to be verified at first if it is possible to lift the strongback up to its final position through the threaded supports. Once the supports are in contact with the strongback, they have to be moved up through their threaded surfaces, one by one.
Therefore FEM simulations have been performed in order to simulate the first step of this lifting process, which is the critical one.

4.2.1 Estimation of the torque and the force

The coldmass weight (28.8 kN) and the gravity are applied as vertical loads. One vertical displacement (2.12 mm) corresponding to a half turn of one threaded support is applied. Till the other seven supports are not lifted up through their threads, they can be considered as unilateral supports. That is the reason why they are modelled as "Compression Only Support". The strongback is fully constrained in the horizontal plane. Because of the symmetry of the strongback just four displacements are applied, one per each simulation (Fig. 8). The values of the forces related to the imposed displacement and to the unilateral supports are obtained from the "Force Reaction" result item. From the force corresponding to the displacement it is possible to estimate the torque necessary to turn the threaded support. The equation adopted to calculate the torque is

$$T = \frac{W d_m}{2} \frac{f \pi d_m + L}{\pi d_m - f L} + \frac{W f_c d_c}{2} \tag{1}$$

where T is the torque, W is the force related to the displacement, d_m is the mean diameter of the thread contact, d_c is the diameter of the collar, L is the lead, f and f_c are the coefficients of static and kinetic friction, respectively.
Eq. 1 is suitable for square thread: even if this is not the case, it can be used without significant error considering the inherent variability in the coefficient of friction. Because of this uncertainty it has been assumed that $f = f_c$ and the value adopted is for a dry contact between steel and stainless steel.
The actual force F to be applied to turn the threaded supports is obtained considering an arm a of 50 cm. Table 1 shows the input data and results of the estimation of torque and force.

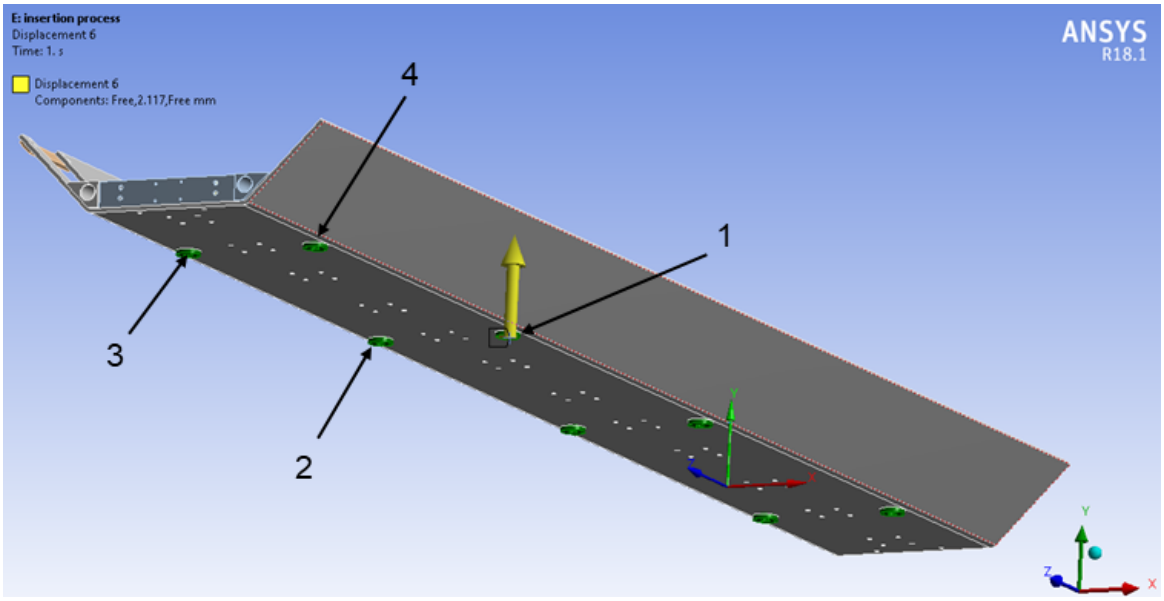

Figure 8: Application of the displacement corresponding to the support in the "1" position

	W [kN]	L [mm]	d_m [mm]	d_c [mm]	f	f_c	a [mm]	T [Nm]	F [N]
1	14.6	4.23	35.4	38.1	0.8	0.8	500	447	894
2	14.4	4.23	35.4	38.1	0.8	0.8	500	439	874
3	9.49	4.23	35.4	38.1	0.8	0.8	500	290	579
4	9.64	4.23	35.4	38.1	0.8	0.8	500	294	588

Table 1: Estimation of the torque and the force

4.3 Force on the pins

The results of Tab. 1 show high values of torque and force. In order to reduce these values it is suitable to make less than a half turn of the threaded supports, for example a quarter turn. Moreover, it is necessary to check the stresses on the components through which the torque is actually transmitted. As shown in Fig. 9, the torque should be applied through four pins, therefore a custom wrench is necessary. FEM simulations are performed to check the stresses on the pins of the wrench and on the corresponding holes of the cylindrical supports. It is considered that just two of the four pins are working at the same time.
A friction coefficient of 0.2 is considered between the pins and the holes and between the flat surface of the support and the wrench (Fig. 9b). The upper surface of the cylinder is constrained as fixed support. A tangential force is applied to the end of the wrench to simulate the tightening process. The values of the force to be applied are indicated in Tab. 1, nevertheless the simulation is performed at first applying a force of 100 N. Even if this value is much lower than the ones of Tab. 1, it causes a maximum stress of 1100 MPa according to the results of the elastic analysis shown in Fig. 10. It is clear then that the pins cannot transmit the force and the torque expected.
Therefore the possibility to modify the shape of the supports has been studied in order to use a standard hexagonal wrench and increase the surface of contact.
Therefore the geometry of the supports are modified as shown in Fig. 11 in order to be fit for a standard wrench. A standard wrench suitable for this application can transmit a torque considerably higher than the ones shown in Tab. 1.

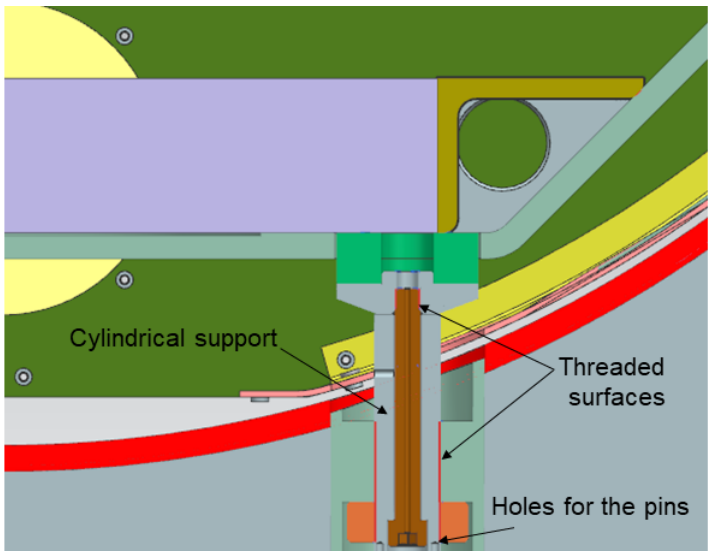

(a) Cross section of the strongback with its supports

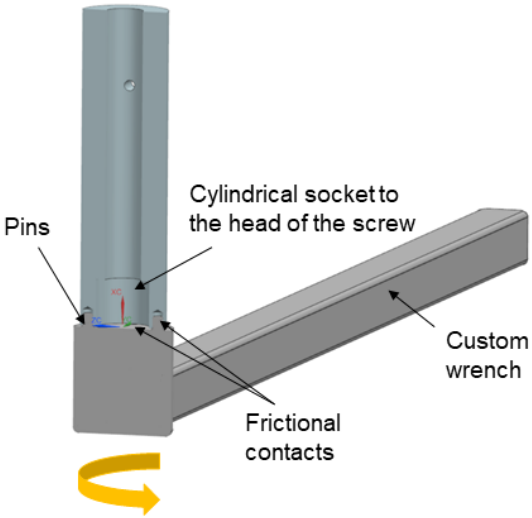

(b) Cross section of a custom wrench connected to the cylindrical support

Figure 9: Detailed geometry of the cylindrical support

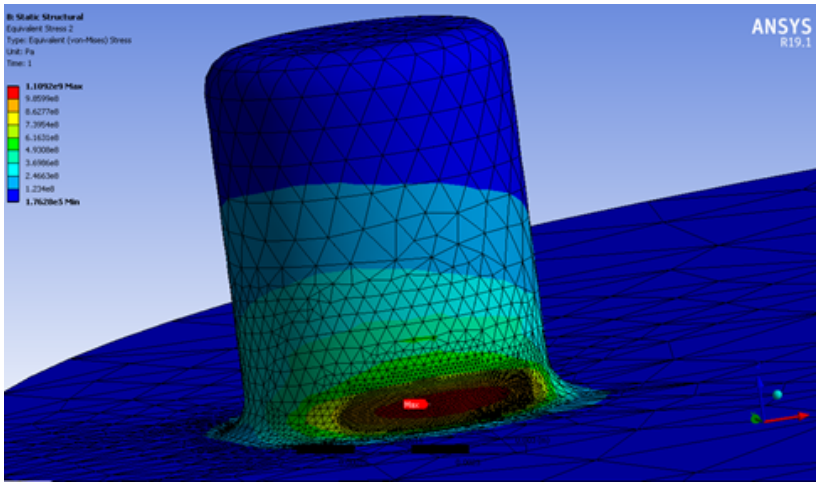

Figure 10: Stress distribution in the pin

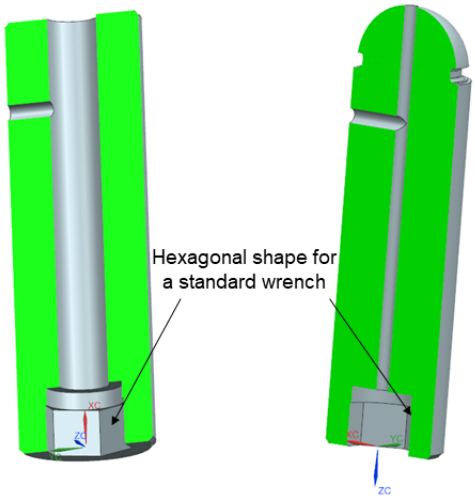

Figure 11: New geometry of the supports

4.4 Design of the roller system

Once validated the idea to lift the strongback turning the threaded supports, the roller system is designed using the NX^{TM} software. The room available for the insertion tooling is quite small as shown in Fig. 12. Note that the magnetic shield plate will be put in place just at the final stage of the insertion process.

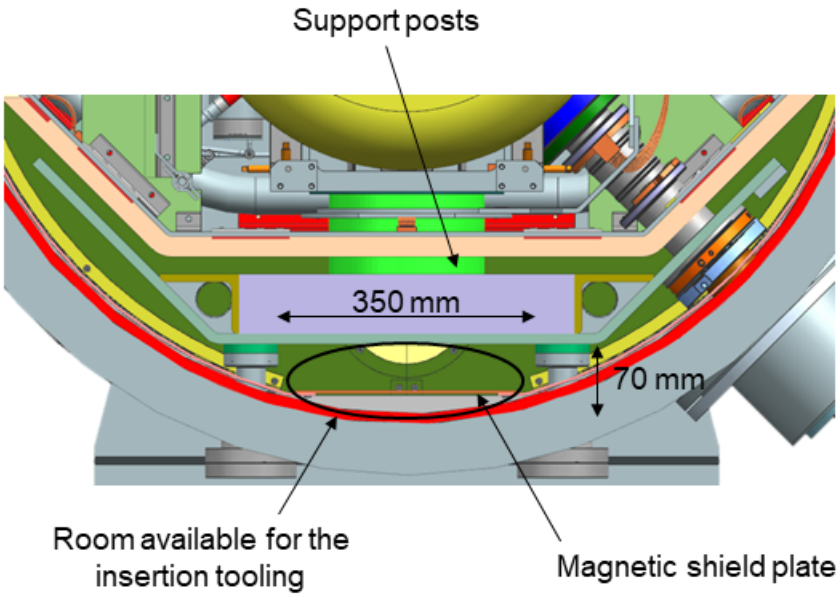

Figure 12: SSR1 cross-section: few room available for the insertion tooling

The main challenge is to fit the tube and rollers in this room, therefore their width should be limited. On the other hand there is an opposite requirement, related to the connection of the roller system to the strongback. It is required to have a wider surface through which the screws can penetrate, avoiding any interference with the support posts. One possible solution is the one illustrated in Fig. 13: there is a main tube which is no more a full-length one because two other tubes are welded at its ends. The axes of the welded tubes are perpendicular to the main tube axis. These two standard tubes have to be machined for several reasons. First of all two simple holes have to be made for the connection of the roller system to the strongback through screws. In addition some cuts have to be made to have access to these screws. Two other holes, the bigger ones shown in Fig. 14a, are necessary to house the head of the screws that fix the support posts to the strongback.

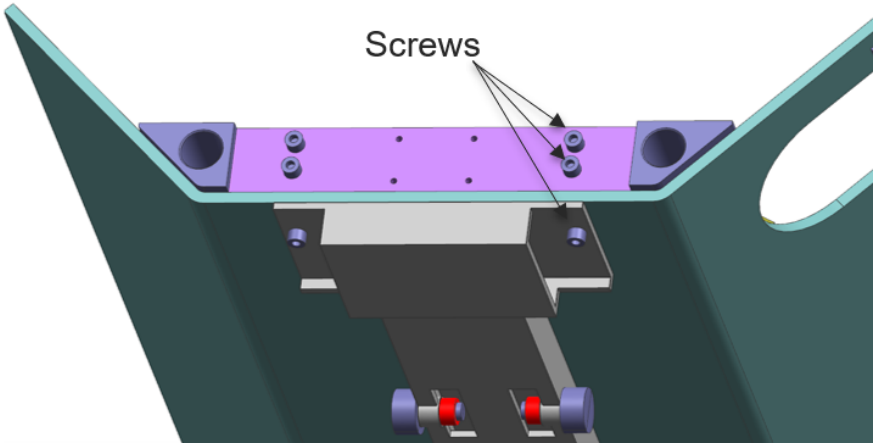

Figure 13: End of the insertion tooling connected to the strongback

It is better to avoid making threaded holes in the aluminum strongback because its thickness is too small. That is the reason why it is planned to do simple holes in the strongback and to fasten the screw on stainless steel L angles (Fig. 14b), two per each end of the strongback. Every angle exhibits three threaded holes: two to fasten the L angles to the strongback and one to fasten, and unfasten when necessary, the roller system to the strongback. After removing the roller system, the angles are kept in place because there is no enough room to extract them once the coldmass assembly is inserted.
As explained before, the tubes present holes in correspondence of the ones shown in Fig. 14b to allow the fastening of the support posts to the strongback.

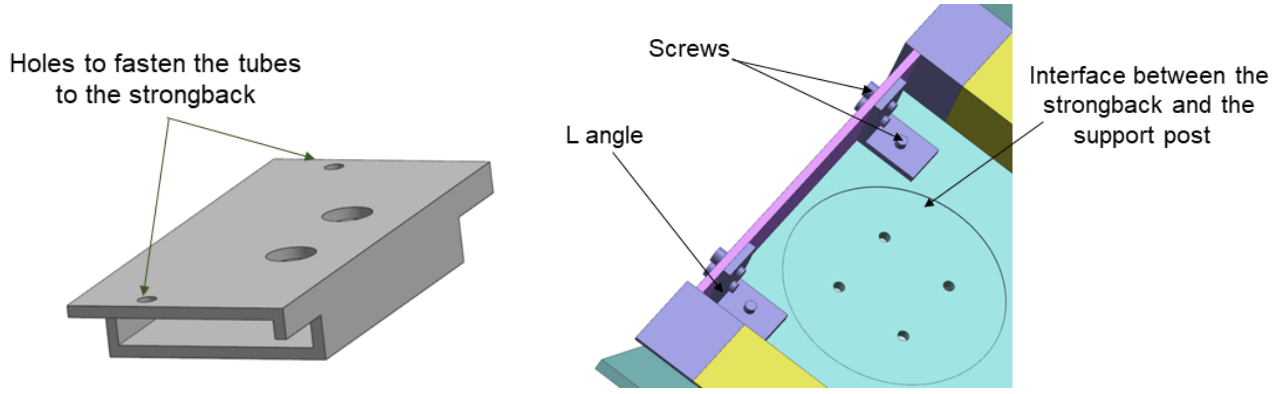

(a) Welded end tube (b) L angle connections

Figure 14: Connection system

The rollers chosen to guide and position the strongback are also known as cam followers. They are based on needle roller bearings. Instead of an inner ring, they have a threaded solid stud. As shown in Fig. 15, the rollers are connected to the insertion tooling thanks to cylindrical tubes welded to the main rectangular tube: the threaded studs of the rollers are fastened to the threaded inner diameter of the cylindrical tube and are secured with nuts at the ends.

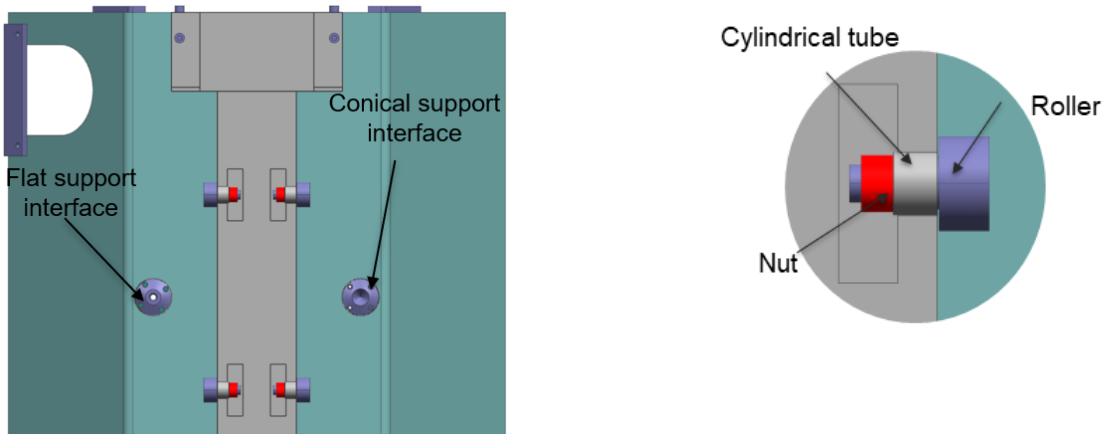

(a) Bottom view of the roller system connected to the strongback

(b) Simplified geometries of the roller interfaces

Figure 15: Rollers connected to the tube

5 Insertion process

The insertion of the coldmass assembly into the vacuum vessel can be divided into four main steps as shown in Fig. 16. Thanks to the roller system, the strongback slides into the vacuum vessel below its final position (Fig. 16a). Then, the eight supports are moved up until they touch the strongback (Fig. 16b). The four screws connecting the insertion tooling to the strongback are unfastened (Fig. 16c), and then the strongback is moved up above its nominal position to allow removing the insertion tooling. Finally, the magnetic shield plate is put into place and the strongback is lowered down to its nominal position (Fig. 16d).

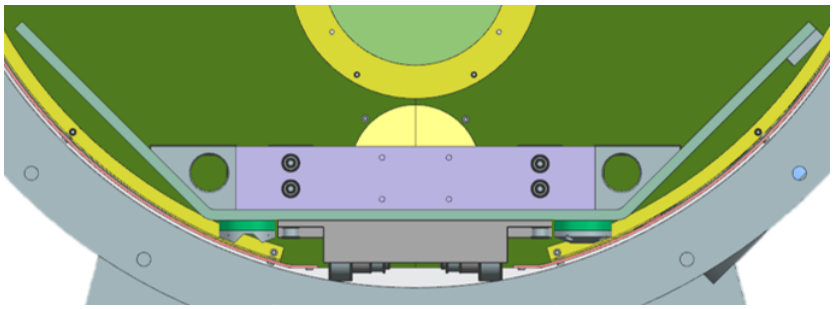

(a) Step 1

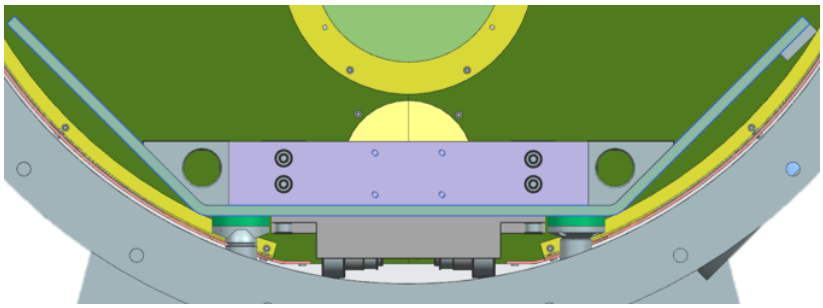

(b) Step 2

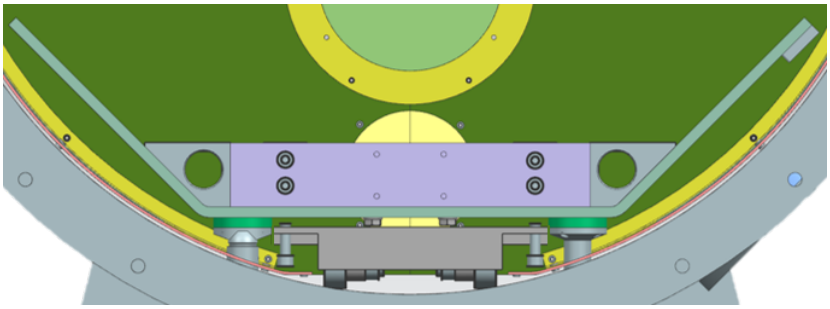

(c) Step 3

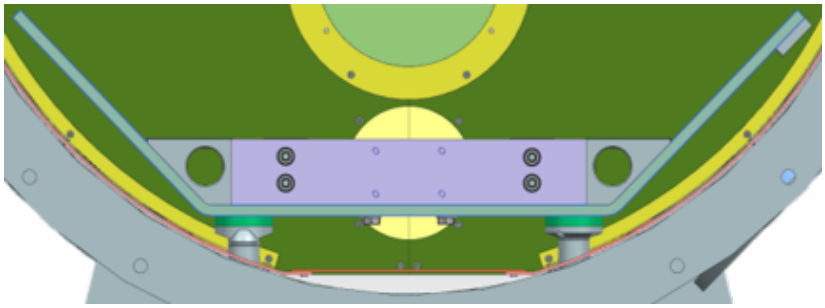

(d) Step 4

Figure 16: Main phases of the SSR1 cryomodule assembling procedure

5.1 Clearances

The design of the insertion tooling is such that it is possible to go through all the steps of the insertion procedure keeping enough clearance between the components. Steps 1 and 3 are the critical ones. Both the insertion tooling and the support interfaces are designed to allow a clearance of 4 mm between the support interfaces and the magnetic shield during the first step of the insertion (Fig. 17a). It is also important to pay attention to step 3, especially to the sizes and dimensions of the head of the screws which fix the support posts to the strongback. Before the removal, the strongback has to be moved up enough to guarantee a cleareance between the head of the screws and the upper part of the insertion tooling as shown in (Fig. 17b). Note that there is enough clearance between the top of the coldmass and the vacuum vessel (around 20 mm). Therefore, it will be possible to lift the coldmass as needed in order to remove the insertion tooling.

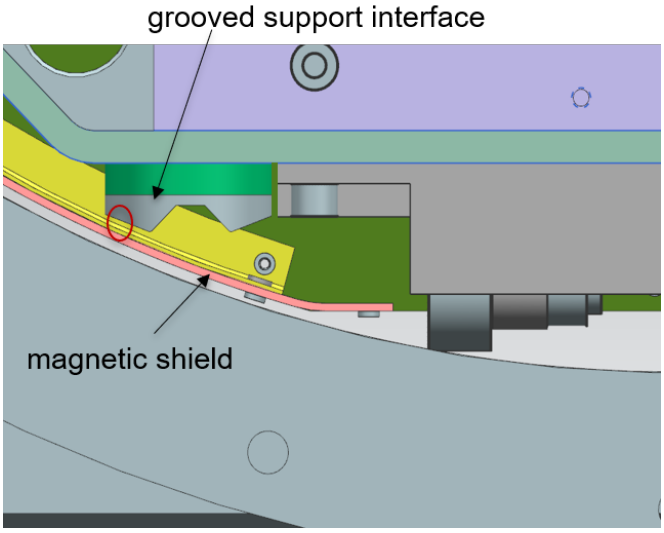

(a)

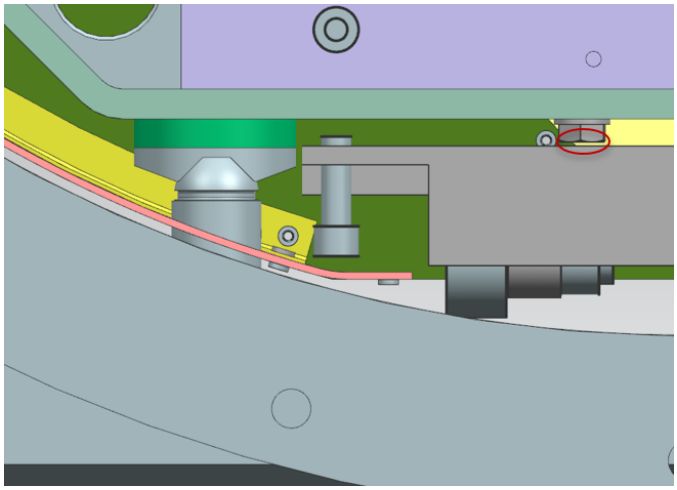

(b)

Figure 17: Clearances in steps 1 and 3

5.2 Contact with the support interfaces

5.2.1 Elastic analysis

In order to guarantee suitable clearance in Step 1, the support interfaces have been modified by reducing their thickness. Therefore, these components become weaker and FEM simulations have to be performed in order to check the stresses in the thinner part.
There are three types of contact depending on the geometry of the supports and of the support interfaces. The upper support surface can be both spherical or flat while the interfaces present a flat, conical or V-shaped surface. The eight types of contact between supports and support interfaces are respectively: spherical surface with V-shaped surface (one), spherical surface with conical surface (one), flat surface with flat surface (six). Of all the three types of contact just the first one is verified because it presents single points of contact in theory, therefore it is the most critical.
A quarter model of three components is implemented as shown in Fig. 18a. The three components are: the steel spherical support, the AISI 304 stainless steel grooved support interface and the aluminum interface welded to the strongback. In theory there are two single points of contact between the surface of the spherical surface and the flat inner surfaces of the grooved support interface. This type of contact is modelled as a frictionless one. Bonded contacts are used between the two interfaces because their flat surfaces are connected through screws while their inner cylindrical surfaces are threaded and tightened together.
Beyond gravity, half weight of the coldmass and the strongback is considered as actual load acting on one support: especially in the phase of alignment and centering of the strongback, it can be assumed that just the two spherical supports are working and therefore each one holds up half of the whole weight.
The results of the simulation are shown in Fig. 18b: the von Mises stresses in the thinner section are not higher than 75 MPa. Therefore, there are no problems in this area. Nevertheless, according to this elastic analysis, a maximum stress equal to 2356 MPa has been estimated in the contact region.

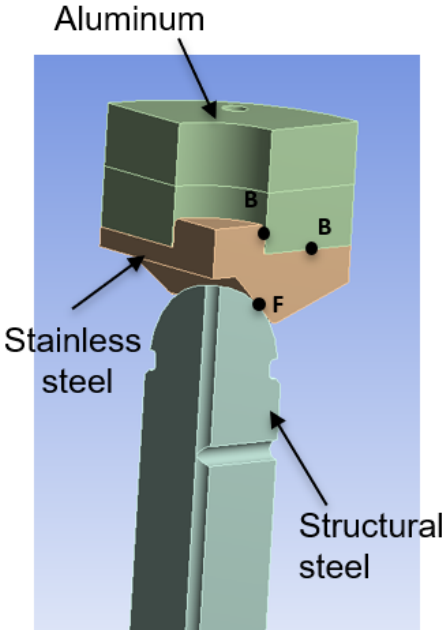

(a) Quarter model with frictionless (F) and bonded (B) contacts

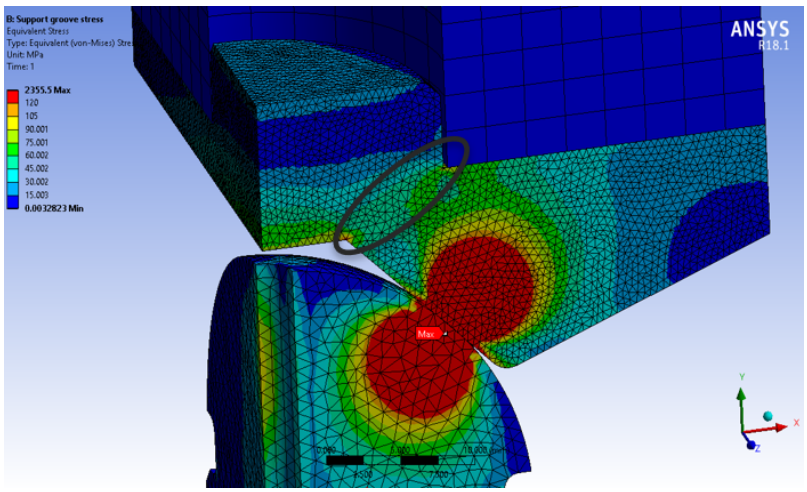

(b) Equivalent stresses do not exceed 75 MPa in the section of interest

Figure 18: FEM analysis of the contact

5.2.2 Elasto-plastic analysis

In order to quantify the stresses and strains in that area it is suitable to switch from an elastic analysis to an elasto-plastic analysis. Just the two components involved in the contact are modelled. A Bilinear Isotropic Hardening material model is used for both pieces, considering a stainless steel yield strength of 205 MPa and a structural steel yield strength of 408 MPa. The tangent modulus is equal to zero in the material model adopted. In this case the analysis performed is non linear due both to the frictionless contact and the material model. An APDL command "ERESX, NO" is used to avoid the extrapolation of integration point results to the nodes. Otherwise the solution shows values over the yield strength and that violates the material model. According to the results of the analysis, the spherical support experiences a maximum equivalent stress of 408 MPa (Fig. 19) and a maximum equivalent strain of 0.002. The maximum equivalent plastic strain is localized and definitely small (2 10^{-4}). On the other hand, the grooved support interface experiences a maximum equivalent stress of 205 MPa and a maximum plastic strain of 0.08 (Fig. 20). The entity of this strain is quite high but, first of all, it should be considered that the worst case has been studied: just the two spherical supports are working. Furthermore, the most common damages due to contact surfaces are induced by a repeated relative surface motion and that is not the case. Therefore, the entity of the compressive strain does not compromise the right functioning of the support.

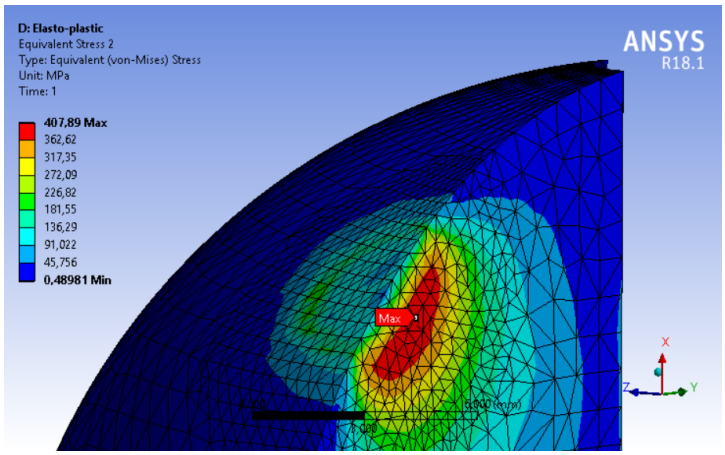

Figure 19: Equivalent stress distribution in the spherical support

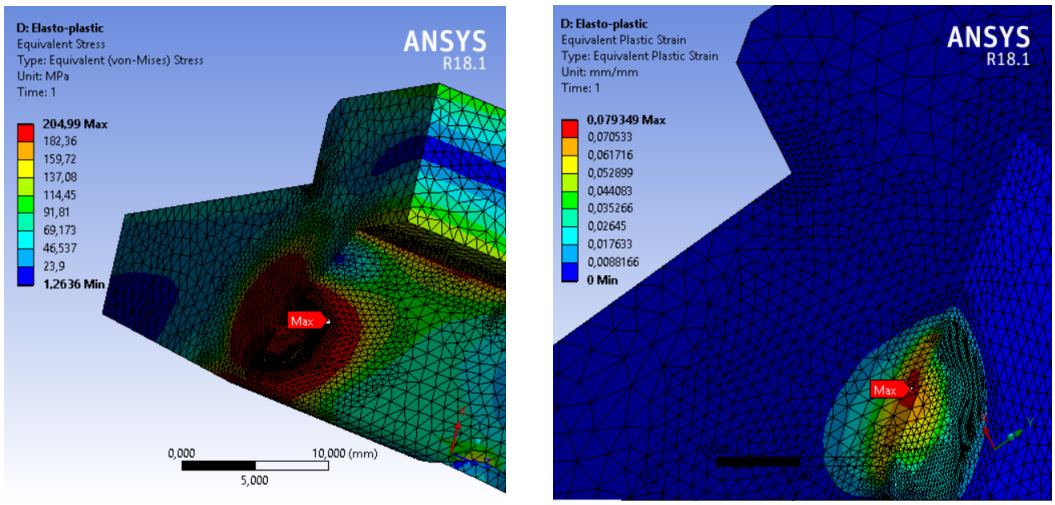

(a) Equivalent stress distribution (b) Equivalent plastic strain distribution

Figure 20: Stress and strain distribution in the grooved support interface

6 Conclusions and further developments

6.1 Achievements

The insertion process of the coldmass into the vacuum vessel of the SSR1 cryomodule has been studied. Over the years different solutions for the insertion were explored; nevertheless calculations have shown that the deflection of the strongback was the main issue. The previous solutions were too risky. Therefore, it has been decided to design a new insertion tooling for which the most important constraint was the small clearance available for the insertion and the removal of the coldmass.
At the same time calculations have been made on the whole system: the strongback and its insertion tooling. At first the values of torque and force necessary to lift up the whole system once in the vacuum vessel have been estimated. Some modifications to the geometry of the supports have been done in order to apply the estimated torque.
Additional FEM analyses have been made to check the stress and strain distribution of the supports and of the support interfaces during the lifting phase. The results have shown that these components experience a local plastic strain near the surfaces of contact. Anyway the entity of the plastic strain does not provoke a significant shape variation of the components.

6.2 Further developments

The next step to validate the new insertion tooling is to perform a step by step simulation of the insertion of the coldmass. In that way it is possible to estimate the pressure on each roller that progressively comes in contact with the cylindrical surface of the vacuum vessel. Rollers can be mounted with their axes inclined in order to avoid a theoretical single point of contact between them and the surface of the vessel. Otherwise the circular external surface of the rollers can be machined in order to have a little surface of contact and not just a single point.
The step by step simulation of the insertion would be useful also to estimate the number of rollers necessary for this application, taking into account the maximum radial and axial load they can support. These values can be obtained from catalogs considering that standard rollers will be used.
It should also be considered the possibility to change the end parts of the roller system: instead of three rectangular tubes welded together it is possible to have just a full-length tube. This one has to be machined at the ends and a wider plate for each end has to be welded to the tube. This change does not modify the concept of this new insertion tooling and all the calculations presented in this report remain the same. Nevertheless this change will make the manufacturing easier.
Taking into account all the problems related to the insertion procedure, it should be considered the idea to develop a completely different strongback shape with wheels directly mounted on it. In this way no insertion tooling will be needed.

References

[1] T. Nicol, S. Cheban, M. Chen, M. Merio, Y. Orlov, D. Passarelli, T. Peterson, V. Poloubotko, O. Pronitchev, L. Ristori, I. Terechkine, P. Bhattacharyya, "SSR1 cryomodule design for PXIE", 2013.

[2] V. Roger, S. Cheban, T. H. Nicol, Y. Orlov, D. Passarelli, P. Vecchiolla, "Design update of the SSR1 cryomodule for PIP-II project", 2018.

[3] D. Passarelli, F. di Ciocchis, M. Parise, V. Roger, "Tooling systems for the assembly and integration of the SSR1 cryomodule for PIP-II project at Fermilab", 2018.

[4] F. Di Ciocchis, D. Passarelli, M. Parise, V. Roger, "Assembly strategy of the 1st SSR1 cryomodule for PIP-II".

[5] V. Poloubotko, "The SSR1 cryomodule coldmass installation fixture", 2018.

[6] Robert C. Juvinall, Kurt. M. Marshek, "Fundamentals of Machine Component Design", John Wiley & Sons Inc., 2000.

[7] C. Santus, "Materiale per la didattica". http://people.unipi.it/static/ciro.santus/Didattica.html.

[8] ANSYS, Inc., "ANSYS Mechanical Structural Nonlinearities- Introduction to contact". http://inside.mines.edu/~apetrell/ENME442/Labs/1301_ENME442_lab6_lecture.pdf.

[9] ANSYS, Inc. "Mechanical User's Guide - SHARCNet". https://www.sharcnet.ca/Software/Ansys/16.2.3/en-us/help/wb_sim/ds_Home.html.

[10] "Proton Improvement Plan-II". https://http://pip2.fnal.gov.

[11] "Tap Chart UNC/UNF Threads". http://www.carbidedepot.com/formulas-tap-standard.html.

[12] "McMaster-Carr". https://www.mcmaster.com.

[13] Bondhus Corp., "Bondhus Resource Manual", 2012. http://www.bondhus.com/bondhus_products/Bondhus-Resource-1-13-10.pdf.